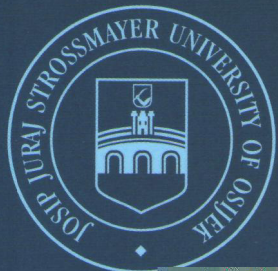


UDK/UDC 62(05) = 163.42 = 111

ISSN 1330-3651 (Print), ISSN 1848-6339 (Online)

Teh. vjesn.



# V TEHNIČKI VJESNIK

## TECHNICAL GAZETTE

# TEHNIČKI VJESNIK TECHNICAL GAZETTE

Znanstveno-stručni časopis tehničkih fakulteta Sveučilišta Josipa Jurja Strossmayera u Osijeku  
Scientific professional journal of technical faculties of the Josip Juraj Strossmayer University of Osijek

Godište (Volume) 20

Broj (Number) 1

Slavonski Brod, siječanj - veljača (January - February) 2013.

Teh. vjesn.

Stranica (Pages) 1-203

**Address of Editorial Office:**

Strojarski fakultet - Tehnički vjesnik  
Trg Ivane Brlić-Mažuranić 2  
HR-35000 Slavonski Brod, Croatia  
Tel.: +385 35 493 423, faks: +385 35 446 446  
e-mail: [tehnvj@sfsb.hr](mailto:tehnvj@sfsb.hr), [technical.gazette@gmail.com](mailto:technical.gazette@gmail.com)  
<http://hrcak.srce.hr/tehnicki-vjesnik>

**Publishers:**

Technical faculties of the Josip Juraj Strossmayer University of Osijek (UNIOS):  
Mechanical Engineering Faculty in Slavonski Brod (MEFSB) (Strojarski fakultet u Slavonskom Brodu); Faculty of Electrical Engineering Osijek (FEEOS) (Elektrotehnički fakultet Osijek) and Faculty of Civil Engineering Osijek (FCEOS) (Građevinski fakultet Osijek)

**Supporting institution:**

Polytechnic of Slavonski Brod (PSB) (Veleučilište u Slavonskom Brodu)

**Council of Journal:**

Damir MARKULAK (FCEOS), Chairman; Radoslav GALIĆ (FEEOS), Member;

**Computer Typesetting and Screen Break:**

Intes, 35000 Slavonski Brod, Nas. Slavonija 2-6/3  
tel./faks: +385 35 447 426

**Print:**

Grafika d.o.o., 31000 Osijek, Strossmayerova 295  
tel.: +385 31 310 300, fax: +385 31 310 303

All papers published in journal have been reviewed.

**Journal published bimonthly.**

(From No. 1, Vol. 20, January – February, 2013)

Circulation: 500 issues

**Journal is referred in (Abstracting and Indexing):**

Science Citation Index Expanded (Web of Science) and Journal Citation Reports/Science Edition (from January, 2008); SCOPUS; INSPEC; COMPENDEX; Ei-Compendex; Geo Abstracts (Civil Engineering, Process Engineering and FLUIDEX) (DIALOG, ESA/IRS); Cambridge Scientific Abstracts

## Contents

## Sadržaj

	<b>Preface</b>	III
	Uvodna riječ	
<b>Original scientific paper</b> Izvorni znanstveni članak	<i>Cagatay Catal, Banu Diri</i> <b>A fault detection strategy for software projects</b> Strategija otkrivanja pogrešaka za projekte softvera	1
	<i>Miroslav Demić, Jasna Glišović, Danijela Miloradović, Jovanka Lukić</i> <b>Contribution to identification of mechanical characteristics of passenger motor vehicle's drum brakes</b> Doprinos identifikaciji mehaničkih karakteristika bubanj kočnica putničkih motornih vozila	9
	<i>Robert Čep, Adam Janásek, Lenka Čepová, Jana Petrů, Ivo Hlavatý, Zlatan Car, Michal Hatala</i> <b>Experimental testing of exchangeable cutting inserts cutting ability</b> Eksperimentalno ispitivanje rezne sposobnosti izmjenjivih reznih umetaka	21
	<i>Damir Kakaš, Pal Terek, Aleksandar Miletić, Lazar Kovačević, Marko Vilotić, Branko Škorić, Dragomir Krumes</i> <b>Friction and wear of low temperature deposited TiN coating sliding in dry conditions at various speeds</b> Trenje i trošenje nisko temperaturno nanese TiN prevlake klizanjem u suhim uvjetima pri različitim brzinama	27
	<i>Jose R. Hílera, Luis Fernandez-Sanz, Sanjay Misra</i> <b>Present and future of Web content accessibility: An analysis</b> Sadašnjost i budućnost dostupnosti sadržaja Web-a: analiza	35
	<i>Marinko Stojkov, Mirza Atić, Adamir Jahić</i> <b>Initial current reduction of synchronous motors with salient poles by static converters usage</b> Smanjenje struje pokretanja sinhronih motora s istaknutnim polovima pomoću statičkih pretvarača	43
	<i>Lidija Tadić, Tamara Dadić, Branimir Barać</i> <b>Flood frequency modelling of the Kopački rit Nature Park</b> Modeliranje učestalosti plavljenja Parka prirode Kopački rit	51
	<i>Boris Jerman, Anton Hribar</i> <b>Dynamics of the mathematical pendulum suspended from a moving mass</b> Dinamika matematičkog njihala koje visi na pomičnoj masi	59
	<i>Mirko Djapic, Ljubomir Lukic</i> <b>Application of Dempster-Shafer theory in conceptual design of the machining centres</b> Primjena Dempster-Shafer teorije u konceptijskom projektiranju obradnih centara	65
	<i>Željko Hederić, Damir Šoštarić, Goran Horvat</i> <b>Numerical calculation of electromagnetic forces in magnetic actuator for use in active suspension system for vehicles</b> Numerički izračun elektromagnetskih sila u magnetskom izvršnom članu za uporabu u aktivnom ovjesu vozila	73
	<i>Ivica Kožar, Neira Torić Malić</i> <b>Spectral method in moving load analysis of Kirchhoff-Love plates</b> Spektralna metoda u analizi Kirchhoff-Love ploča	79
	<i>Dragan B. Đurđević, Momčilo D. Miljuš</i> <b>The procedure proposal for order pick area design</b> Prijedlog procedure za projektiranje komisije zone	85
	<i>Zoran Kovač, Goran Knežević, Danijel Topić</i> <b>Modelling of power system reliability assessment</b> Modeliranje elektroenergetskog sustava za analizu pouzdanosti	93
	<i>Péter Iványi</i> <b>Numerical investigation of semi-rigid column bases with hysteresis characteristics</b> Numeričko ispitivanje polu-krutih temelja stupova s karakteristikama histereze	99
	<i>Aco Antić, Dražan Kozak, Borut Kosec, Goran Šimunović, Tomislav Šarić, Dušan Kovačević, Robert Čep</i> <b>Influence of tool wear on the mechanism of chips segmentation and tool vibration</b> Utjecaj trošenja alata na mehanizam segmentacije odvojenih čestica i vibracije alata	105
	<i>Biserka Runje, Marijan Marković, Dragutin Lisjak, Srđan Medić, Živko Kondić</i> <b>Integrated procedure for flatness measurements of technical surfaces</b> Integrirani postupak ispitivanja ravnosti tehničkih površina	113
	<i>Primož Kržič, Franci Pušavec, Janez Kopač</i> <b>Kinematic constraints and offline programming in robotic machining applications</b> Kinematička ograničenja i izvanmrežno programiranje kod robotskih obradnih programa	117

## Contents

## Sadržaj

<b>Original scientific paper</b> Izvorni znanstveni članak	<i>M. Jasim Uddin, Anis N. Nordin, M. B. I. Reaz, Mohammad Arif Sobhan Bhuiyan</i> <b>A CMOS power splitter for 2,45 GHz ISM band RFID reader in 0,18 <math>\mu</math>m CMOS technology</b> CMOS razdvajač snage za 2,45 GHz čitač polja ISM RFID u 0,18 $\mu$ m CMOS tehnologiji	125
	<i>Robert Pospichal, Gerhard Liedl</i> <b>Simulation of periodic nanostructures fabricated by multi-beam interference of an ultra-short pulse laser</b> Simulacija periodičnih nanostrukture dobivenih interferencijom multi snopa lasera ultra kratkog impulsa	131
	<i>Ante Čikić, Ivan Samardžić, Antun Stoić</i> <b>A contribution to the development of moisture measuring of vacuum-dried hygroscopic materials</b> Doprinos razvoju mjerenja vlage higroskopskih materijala sušenih u vakuumu	137
	<i>Ioan Hiticas, Daniel Marin, Liviu Mihon</i> <b>Modelling and operational testing of pulse-width modulation at injection time for a spark-ignition engine</b> Modeliranje i operativno testiranje modulacije širine impulsa kod vremena ubrizgavanja za motor paljen pomoću svjećice	147
	<i>Ivana Mekjavić</i> <b>Damage identification of bridges from vibration frequencies</b> Utvrdjivanje oštećenja mostova na osnovi vlastitih frekvencija	155
<b>Preliminary notes</b> Prethodno priopćenje	<i>Endri Garafulić, Branko Klarin</i> <b>Acceptable concept of carbon dioxide storage</b> Prihvatljivi koncept pohrane ugljikovog dioksida	161
	<i>Nataša Turina, Diana Car-Pušić, Mladen Radujković</i> <b>Possibilities and limitations of constructability concept in construction industry in Croatia</b> Mogućnosti i ograničenja implementacije koncepta izgradivosti u građevinskoj industriji u Hrvatskoj	167
	<i>Draško Tomić, Dario Ogrizović, Zlatan Car</i> <b>Cloud solutions for high performance computing: oxymoron or realm?</b> Super računalstvo u oblacima: oksimoron ili realitet?	177
<b>Subject review</b> Pregledni članak	<i>Zoran Anišić, Ivica Veža, Nikola Suzić, Nemanja Sremčev, Anja Orčik</i> <b>Improving product design with IPS-DFX methodology incorporated in PLM software</b> Unapređenje konstrukcije proizvoda s IPS-DFX metodologijom ugrađenom u PLM softver	182
	<i>Željko Hećimović</i> <b>Relativistic effects on satellite navigation</b> Relativistički utjecaji na satelitsku navigaciju	195
<b>Appendices</b> Prilozi	<b>Curiosities (Zanimljivosti)</b>	V
	<b>Instructions for authors (Naputak autorima)</b>	XV

# CONTRIBUTION TO IDENTIFICATION OF MECHANICAL CHARACTERISTICS OF PASSENGER MOTOR VEHICLE'S DRUM BRAKES

*Miroslav Demić, Jasna Glišović, Danijela Miloradović, Jovanka Lukić*

Original scientific paper

Based on the conducted analyses, it has been proven that there is no generally accepted method for evaluation of characteristics and output parameters of drum brake mechanisms. Experimental research of the drum brake subsystem with brake fluid pressure in the brake cylinder as input quantity and brake torque as output quantity is presented in the paper. The obtained results show that there is a time delay between the output and input due to the response of the drum brake mechanism. This points to the deficiency of determination of brake performance in time domain, because, in comparison, excitation and response of the system are not adequate. Hence, the dynamic mode is observed in the analysis of the drum brake subsystem. Dynamic analysis determines the behaviour of the system in transient period. With previously known transfer characteristics of a system, its response can be determined in relation to the specified inputs (excitations), which is a good basis for determination of correlation between the results obtained by different methods of identification and under different test conditions.

**Keywords:** data processing, drum brakes, experimental research, mechanical characteristics

## Doprinos identifikaciji mehaničkih karakteristika bubanj kočnica putničkih motornih vozila

Izvorni znanstveni članak

Na temelju provedenih analiza, dokazano je da ne postoji opće prihvaćena metoda ocjene karakteristika i izlaznih parametara mehanizama bubanj kočnica. U radu su prikazana eksperimentalna istraživanja podsustava bubanj kočnica s ulaznom vrijednosti-tlakom kočione tekućine u cilindru kočnice i izlaznom vrijednosti-kočnim momentom. Dobiveni rezultati su pokazali da je između izlaza i ulaza postojalo vrijeme kašnjenja, zbog odgovora mehanizma bubanj kočnice. To ukazuje na nedostatak utvrđivanja performansi kočnica u vremenskoj domeni, jer u usporedbi nisu adekvatna uzbuda i odgovor sustava. Stoga se u analizi podsustava bubanj kočnice promatra dinamički mod. Dinamička analiza određuje ponašanje sustava u prijelaznom razdoblju. Uz već poznate prijenosne karakteristike sustava, njegov odgovor može biti određen u odnosu na navedene ulaze, uzbude, što je dobar temelj za određivanje korelacija između rezultata dobivenih različitim metodama identifikacije i pod različitim uvjetima ispitivanja.

**Ključne riječi:** bubanj kočnice, eksperimentalna istraživanja, mehaničke karakteristike, obrada podataka

## 1 Introduction

The main task of the brake mechanisms is to achieve the required brake torque acting on the wheels of the vehicle, causing their slowing down, and thus braking of the vehicle. Therefore, the brake torque is a fundamental characteristic of every brake, the measuring tool of its functional properties or performances. Operating characteristic of the brake, which is often called the brake factor  $C^*$ , links the activation force of hydraulic piston and brake torque as input and output values and includes all structural parameters of the brake and the available friction factor between the friction surfaces.

Vehicle design concept with disc brakes on the front wheels and drum brakes on the rear wheels enables manufacturers to continue providing most of the advantages of disc brakes, in addition to low production costs. Drum brakes are less expensive to produce than disc brakes, mostly because they can also operate as parking brakes, while disc brakes require a special parking brake mechanism [1].

The importance of the drum brakes comes from the fact that, in 2011, drum brakes were fitted to 45 per cent of new cars globally. This figure is set to remain above 40 per cent for the next five years, with statistics indicating that over 40 million new cars will be fitted with drum brakes at registration in 2016. Smaller cars that use drum brakes are becoming more popular, driven by both the economy and the need to reduce emissions. Since 2008, the average engine size of new cars at registration has been downsized across Europe. Sometimes viewed simply as an old technology, the drum brakes are still the most

cost effective solution for rear brakes in the vast majority of cars. There is also a dangerous misconception that the rear brakes are not as important as the front brakes, as the front brakes provide up to 80 % of the braking force. Even though the rear brakes contribute with less braking force, they still have a large impact on the stability of a car [8].

Calculation methods and testing procedures for drum brake mechanisms, present in a large number of papers, have passed through several stages in their development. Classic analytical design methods are based on a number of simplifications that significantly reduce the accuracy of the results [2, 3]. The utmost assumptions are to ignore elasticity of the drum and friction lining and to idealize pressure distribution on the friction surface [4]. Calculation methods have experienced intense development thanks to the development of computer techniques. In this way, numerical methods have become the basic calculation methods, without which it cannot be possible to imagine the development of many products today, in technologically advanced countries. These methods allow rapid analysis of many different combinations and selection of the optimal solution (optimization). Numerical methods [5, 6, 7] are approximate and require reliable information on which the boundary conditions are derived. From this, their direct link with the testing of brake mechanisms comes, that provides information of high precision and quality, thanks to the advancement of measurement and processing techniques and analysis of measurement results. In this way, the period needed for the development of new brakes' elements is significantly



reduced. A large part of the brake system testing is the verification of compliance with the requirements of international and national regulations. Developmental researches are very diverse and they are necessary for the introduction of a new product or improvement of the existing products.

The conducted analysis shows that there are different research approaches and there is no generally accepted method for evaluation of properties and output parameters of drum brake mechanisms. This paper presents one way of defining the criteria for evaluation of mechanical properties of drum brakes for motor vehicles, which includes the phase of experimental measurements and the subsequent processing of recorded data.

## 2 Experimental method

In this paper, the experimental results [10] are used and a corresponding data analysis in frequency domain is performed.

Simplex type of drum brake is mounted at the rear wheels of the tested passenger vehicle. Brake shoes of this simplex brake are supported on the bevel surface with respect to the vertical axis of the brake ("floating" shoes) and they are better adjusted to the drum and provide more even wear of lining. During the braking process, the brake torque which tends to slow down the drum is developed. At the same time, the torque equal in magnitude and opposite in direction acts and transmits to the shoes, seeking to turn them around in the direction of rotation. This torque, which is identically equal to the intensity of the brake torque, is transferred through the shoe's supports and brake cylinders to anchor plate made of sheet metal [9].

The block diagram of the drum brake with the input - brake application pressure in the brake cylinder of the wheel ( $p$ ) and the output - brake torque ( $M_k$ ) is presented in Figure 1 [10].

During the analysis of the observed system, the dynamic mode is observed. The behaviour of the system in the transient regime (process of system's transition from one stationary state to another stationary state) is determined. The mathematical model describes the dynamic operation mode and components of the system and takes into account the time variation of input and output parameters [11].

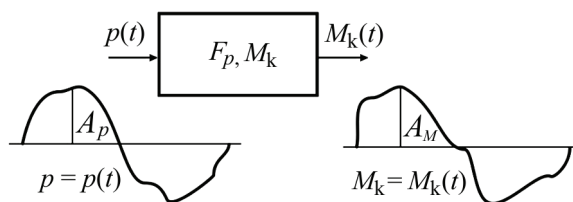


Figure 1 Block diagram of the drum brake

### 2.1 Measurement of pressure in the brake cylinder of drum brakes

During the identification of the mechanical characteristics of drum brake, changes of brake application pressure in the brake cylinder of rear wheels were measured. The hydrostatic brake system was applied

on the tested vehicle in which the command is transmitted from the brake pedal through pipes and hoses to the brake cylinders. This pressure forms the activation forces on the brake piston, i.e. piston rods of brake cylinders that activate the brakes. Constructive limitations prevent the installation of absolute pressure transducer HBM P3MA directly on the brake cylinder of drum brakes. By using especially built-in adapter, the transducer is mounted very close to the brake cylinder, assuming that there is a very small pressure drop along this short distance. The photograph of the mounted transducer P3MA in the brake line of the tested vehicle is given in Fig. 2 [10].

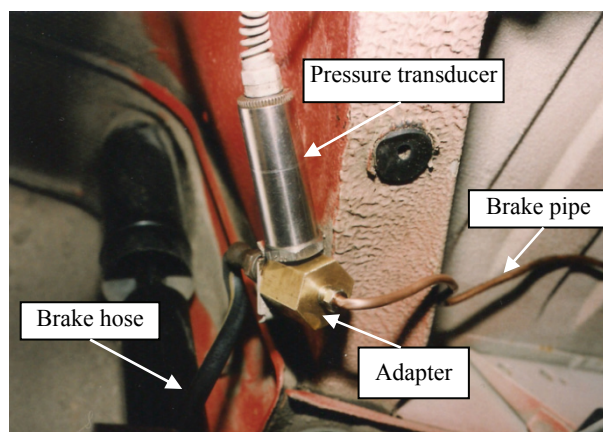


Figure 2 Mounting of pressure transducer P3MA in the brake line

### 2.2 Measuring of the drum brake's torque at independently suspended rear wheels

Drum brake is a complex system consisting of a large number of elements with different characteristics. Viscous losses, mechanical friction and oscillatory system with specific rigidity may occur in the transmission path of the brake torque. All this leads to some losses, so, at the end, the developed brake torque,  $M_k$ , is not equal to the torques in different measurement points. Therefore, during the selection of measurement point for measuring the brake torque, special attention should be given to the fact that by moving away from the friction contact between lining and drum, the measurement error is increasing.

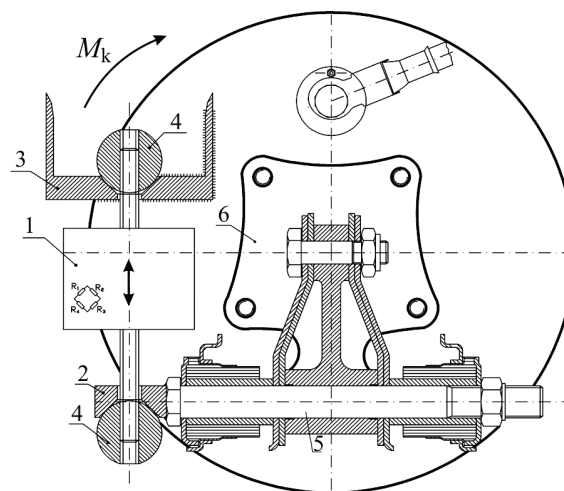


Figure 3 Schematic display of measuring of brake torque indirectly, using the force transducer (1 – Force transducer with strain gauges, 2 – Lower joint's socket, 3 – Upper joint's socket, 4 – Joints, 5 – Screw and 6 – Wheel spindle)

For the purpose of this study and in the absence of a commercial wheel torque transducer (measuring hub) whose price is very high at the market, the prototype of measuring device meeting all the requirements in the field of brake testing was used.

The torque is measured indirectly by the force transducer (Fig. 3). The extension force is measured by strain gauges connected in a full Wheatstone bridge in the transducer. The newly formed transfer path of transmitting the torque enables the entire brake torque to transfer from the anchor plate to the screw connecting the wheel spindle and the shock absorber and swinging arm over to the force transducer. Deformation of the wheel spindle and other losses in the system may be considered negligible. The ends of the transducer are attached by screws to the joints that recline in conical sockets. In this way, the joint connection is achieved which is necessary for force transducer to be exposed to extension and not to bending.

Basic features of this solution for brake torque transducer are:

- the force transducer registers only brake torque,
- the entire brake torque is transmitted through the force transducer, causing extension stress,
- the measuring point in this transducer solution is related to the existence of measurement error due to losses in the transmission of brake torque, which must be taken into account when analysing the results of the experiments,
- the measuring system is not symmetrical (installation of transducer and transmission of load).

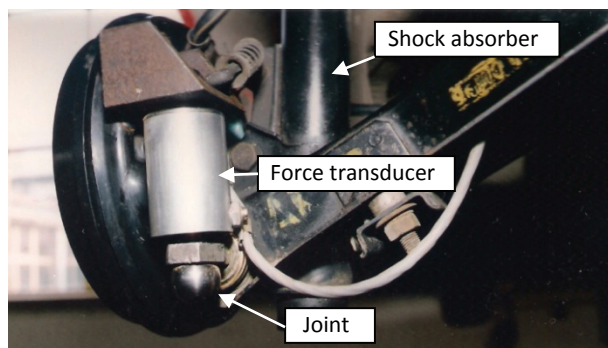


**Figure 4** Mounting of the drum brake torque transducer on the test vehicle

Mounting of brake torque transducer on the brake drum of tested vehicle is shown in the photograph in Figure 4.

Calibration of developed braking torque sensor is done in the laboratory and on the vehicle. The procedure was as follows:

- force transducer with joint connections and anchor plate with welded mount were built in drum brake assembly,
- drum brake assembly is built on the test vehicle,
- shock absorber was placed with its lower end on the support block,
- activation of the brake by pressing the brake command has secured sufficient pressure in the brake cylinder of drum brakes to move apart brake shoes, bring them into contact with the drum and prevent its rotation (the drum was blocked),

- the lever was bolted with two screws to the drum and load (braking torque) was applied with the help of cranes,
- the vertical force acting on the lever was recorded by HBM force transducer.

### 2.3 Measurement of the motor vehicle wheel's speed

In addition to the wheel speed, the other significant quantities may be determined, such as: kinematic radius of the wheel, sliding speed, the coefficient of adhesion, etc. Some systems that are installed on contemporary motor vehicles have speed transducers as constituent components of, for example, ABS (the anti-blocking system), ASR (anti-sliding system) and EFI (electronic control of fuel injection) systems. Fig. 5a shows a schematic display of the measuring chain for measurement of the speed of the test vehicle's rear (driven) wheel by using a magnetic non-contact pulse transducer. The photo of the mounted transducer is given in Fig. 5b. Toothed wheel is firmly attached to drum with screws. The toothed wheel has 60 equally distributed teeth. The metal bracket is mounted opposite to Bosch speed transducer, which is attached to the anchor plate. The two existing M6 screws that secure the drum brake cylinder to the anchor plate were used for mounting and securing of the bracket [10].

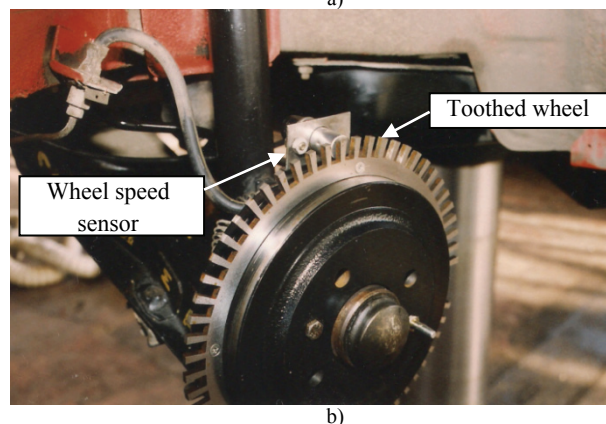
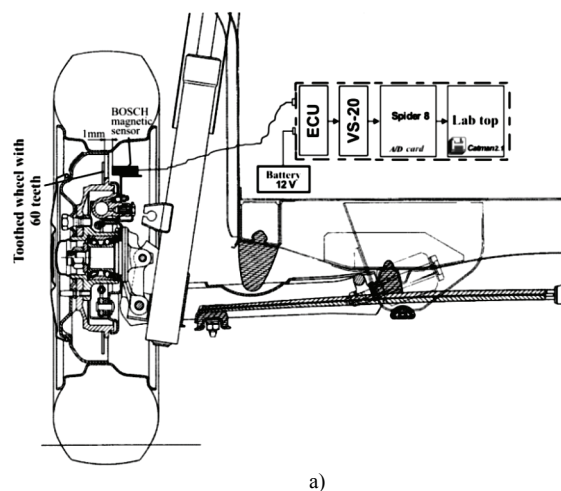


**Figure 5** The components of the measuring set up for recording the rear wheel's speed

Changes of brake line pressure, brake torque and braked wheel's speed were recorded during the braking process until stopping the vehicle, from initial velocities

of 40, 60 and 80 km/h and for ready-to-drive and fully loaded vehicle.

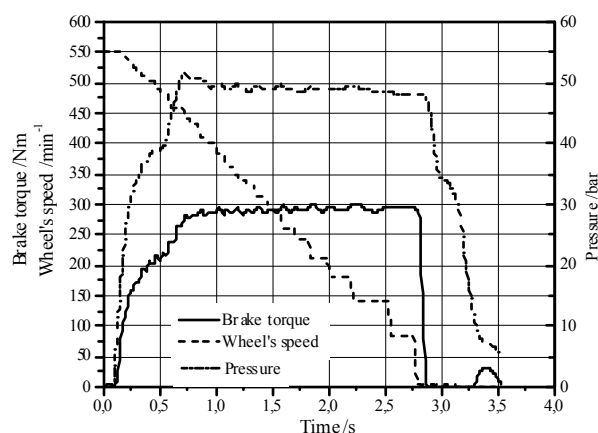


**Figure 6** Change of pressure, brake torque and wheel's speed for a fully loaded vehicle and the initial speed of 60 km/h

The diagrams in Figs. 6 to 9 show the changes in pressure and brake torque in time domain during the braking tests with the disengaged coupling for ready-to-drive and fully loaded vehicle, as well as for different initial velocities of the braking process.

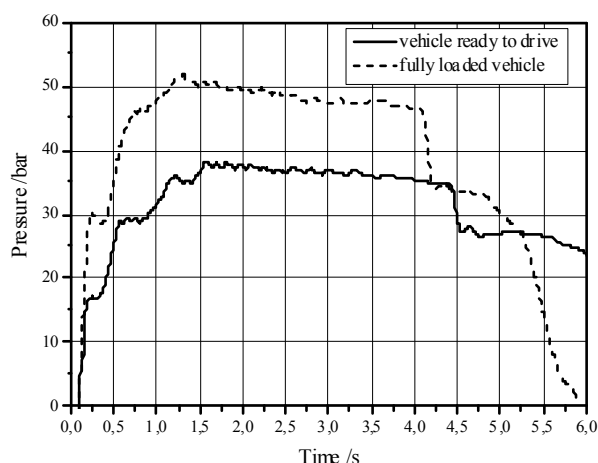


**Figure 7** Influence of the vehicle's weight on the brake application pressure (initial speed 80 km/h)

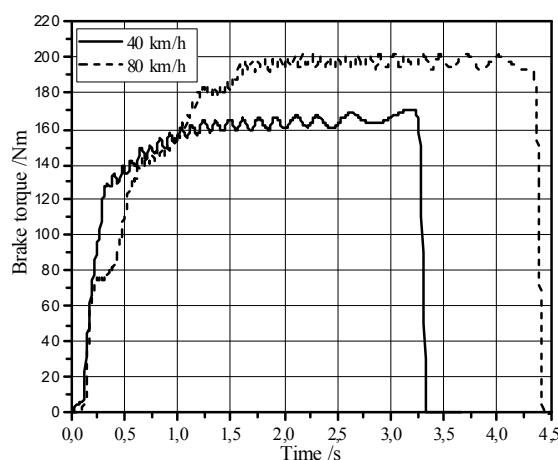


**Figure 8** Influence of the initial vehicle speed on the brake torque (ready-to-drive vehicle)

After the braking test with initial vehicle speed  $v_0 = 40$  km/h, the braking is done with  $v_0 = 60$  km/h and  $v_0 = 80$  km/h. The time period between two braking tests was

about 1 min. The larger increase in brake application pressure and brake torque required to stop a fully loaded vehicle is obvious.

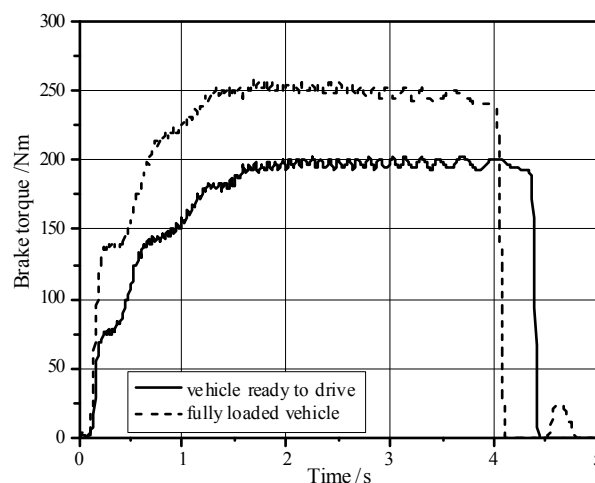


**Figure 9** Influence of the vehicle's weight on the brake torque (initial speed 80 km/h)

Fig. 10 shows the influence of changes of brake application pressure on output values of brake. Change of the brake torque in Fig. 10 shows that, after the end of braking and drop of brake torque to zero, the pressure drop in brake lines happens with some time delay.

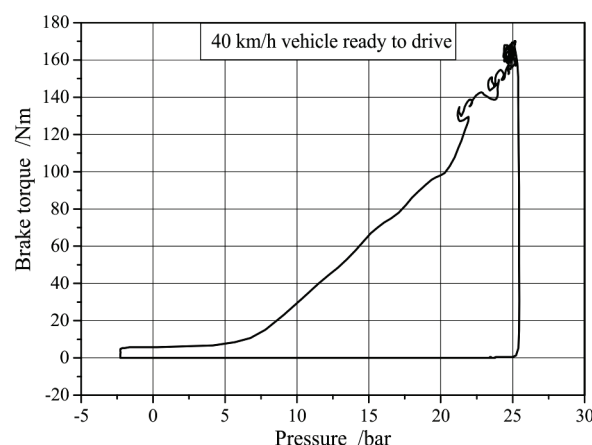


**Figure 10** Brake torque vs. brake application pressure

### 3 Analysis of the experimental results

Preliminary analysis of the recorded signals showed that they belong to the class of the transient processes, and the data processing based on the theory known from [12, 13, 14] was performed.

For the analysis of experimentally recorded data time series, software ANALSIGDEM [15] and DEMPARCOH [16] realized on the basis of the theory known from [12, 13, 14, 17, 18] were used.

During the experimental research, records of the length of 13,639 s with sampling interval,  $\Delta t = 0,00666$  s (sample size was 2048) were registered. Sampling frequency was 150 Hz. In this way, the minimum frequency of 0,0733 Hz and maximum frequency of 75,07 Hz were obtained. Since the resonance frequencies of the system are above 5 Hz, it is obvious that the length of the signals is satisfactory.



For these parameters and for the realized number of averages (524), the statistical errors were calculated by auto and cross-spectral density function calculation. Their values, for the usual technical damping of these systems and the actual resonant frequency are:

- relative "bias" error 0,005,
- relative "random" error 0,043 for single-channel signal and
- relative "random" error for the two-channel signal 0,060, which is quite satisfactory according to [12, 13, 14].

### 3.1 Autocorrelation functions

Figs. 11 and 12 show the obtained autocorrelation functions of brake application pressure and brake torque, respectively.

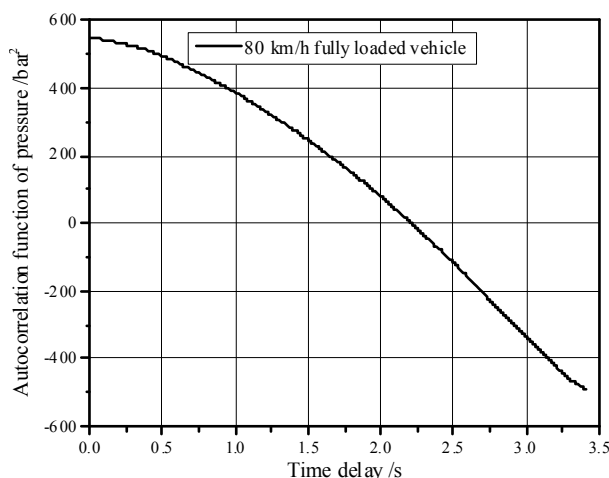


Figure 11 Autocorrelation function of brake application pressure

As an illustrative example, the events that correspond to the initial speed of 80 km/h are shown. It is obvious that the values of autocorrelation functions decrease with respect to the time delay,  $\tau$ . This suggests that the observed processes are transient.

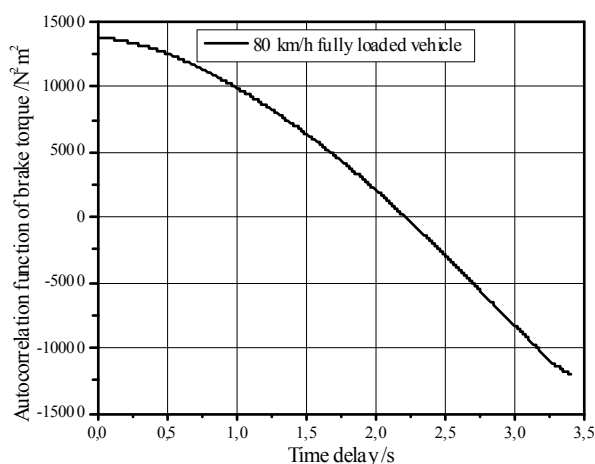


Figure 12 Autocorrelation function of brake torque

### 3.2 Auto spectral density functions

Examples of magnitudes and phases of auto spectral density functions of pressure at initial vehicle speed of 40 km/h for the fully loaded vehicle are given in Figs. 13 and

14. The value of the auto spectral density function magnitude is the largest at low frequency ranges, from 0,18 bar²·Hz ( $f = 8,94$  Hz) to 28,36 bar²·Hz ( $f = 0,15$  Hz). Values of phase vary within the range of  $-1,56$  rad ( $f = 7,33$  Hz) to 1,57 rad ( $f = 5,87$  Hz).

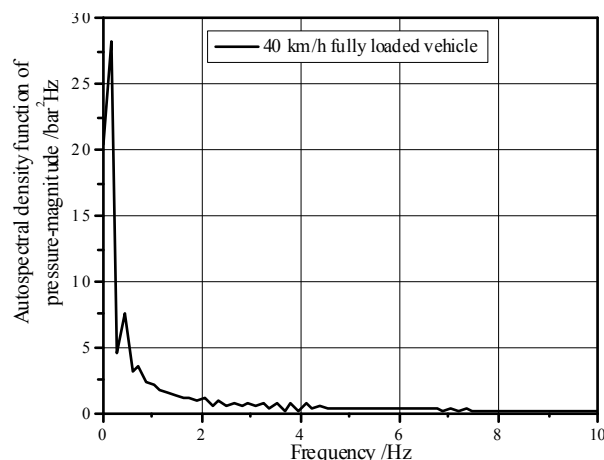


Figure 13 Magnitude of auto spectral density function of the pressure

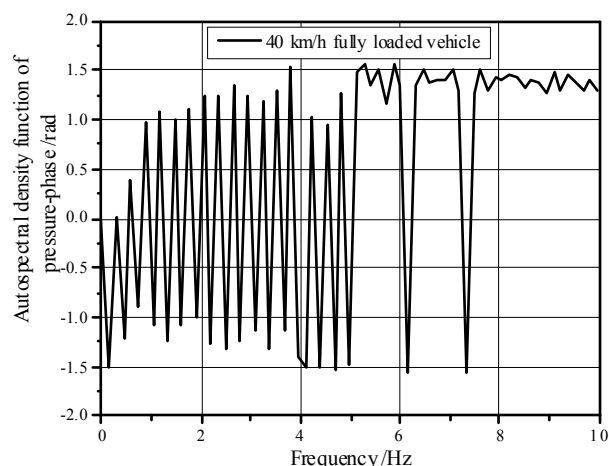


Figure 14 Phase of auto spectral density function of the pressure

The analysis of all obtained data shows that the values of the magnitude of auto spectral density function of the pressure are in the range from 0,01 bar²·Hz ( $f = 7,33$  Hz,  $v_0 = 60$  km/h, fully loaded vehicle) to 30,57 bar²·Hz ( $f = 0,15$  Hz,  $v_0 = 80$  km/h, fully loaded vehicle). The values of phase are within the range from  $-1,57$  rad ( $f = 7,04$  Hz,  $v_0 = 80$  km/h, ready-to-drive vehicle) to 1,57 rad.

Figures 15 and 16 represent examples of magnitudes and the phases of auto spectral density function of brake torque for initial vehicle speed of 40 km/h for the fully loaded vehicle. Values of the magnitude of auto spectral density function of the brake torque are in the range from 0,27 N²·m²·Hz ( $f = 9,82$  Hz) to 146,82 N²·m²·Hz ( $f = 0,15$  Hz). Corresponding phase values are in the range from  $-1,56$  rad ( $f = 6,31$  Hz) to 1,48 rad ( $f = 0,88$  Hz).

The analysis of all obtained data showed that the values of magnitudes of auto spectral density function of the brake torque are in the range from 0,17 N²·m²·Hz ( $f = 7,62$  Hz,  $v_0 = 40$  km/h, ready-to-drive vehicle) to 167,96 N²·m²·Hz ( $f = 0,15$  Hz,  $v_0 = 60$  km/h, fully loaded vehicle). The values of phase are in the range from  $-1,57$  rad ( $f = 2,79$  Hz,  $v_0 = 60$  km/h, ready-to-drive vehicle) to 1,57 rad.

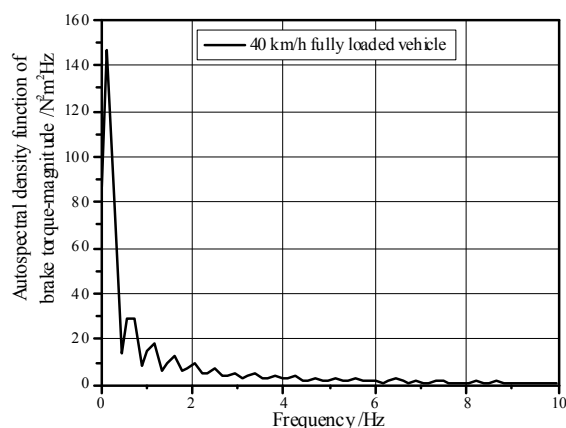


Figure 15 Magnitude of autospectral density functions of the brake torque

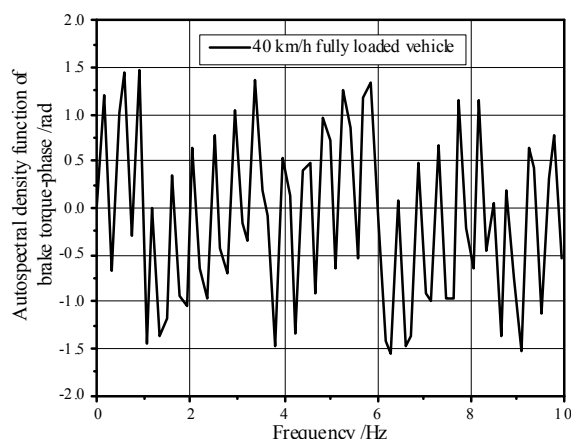


Figure 16 Phase of auto spectral density function of the brake torque

### 3.3 Cross-correlation functions

Maximum values of cross-correlation function between pressure and brake torque for different initial velocities of the braking process are in the range from 66,04 bar·N·m ( $\tau = 0,053$  s,  $v_0 = 60$  km/h, ready-to-drive vehicle) to 239,02 bar·N·m ( $\tau = 0,047$  s,  $v_0 = 60$  km/h, fully loaded vehicle). Time delay is in the range from 0,027 s to 0,06 s.

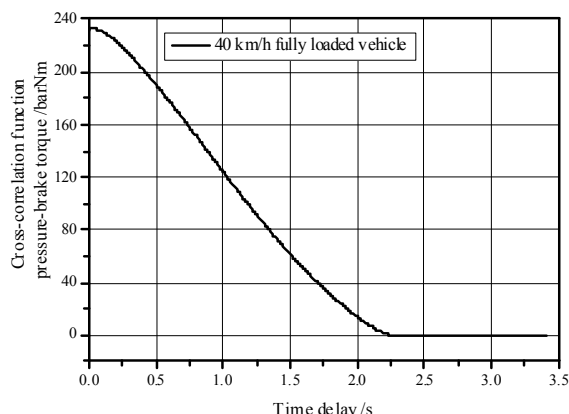


Figure 17 Cross-correlation function between pressure and brake torque

The cross-correlation function between pressure and brake torque for the initial vehicle speed of 40 km/h and fully loaded vehicle is shown in Fig. 17. The maximum value of cross-correlation function is 205,91 bar·N·m and its corresponding time delay is 0,053 s.

Analysis of the influence of vehicle weight and initial velocity on the cross-correlation function between pressure and brake torque is shown in Figures 18 and 19.

It can be noticed that the increase in the vehicle weight (72,96 bar·N·m,  $\tau = 0,053$  s to 205,91 bar·N·m,  $\tau = 0,053$  s) and initial velocity (72,96 bar·N·m,  $\tau = 0,053$  s to 84,92 bar·N·m,  $\tau = 0,006$  s) significantly affects the maximum values of cross-correlation functions between pressure and brake torque. This means that these parameters also affect the parameters of the braking process.

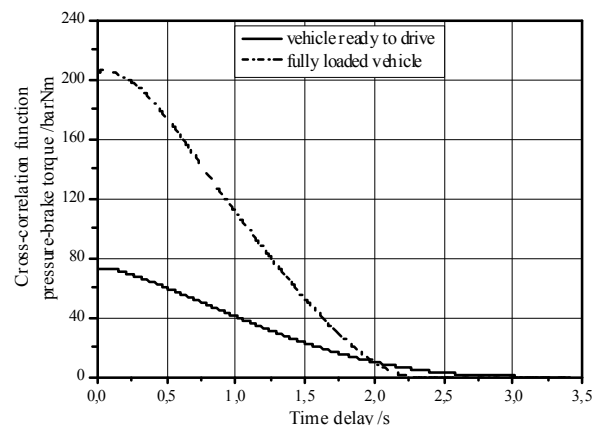


Figure 18 Influence of the vehicle's weight on cross-correlation function between pressure and brake torque (initial vehicle speed 40 km/h)

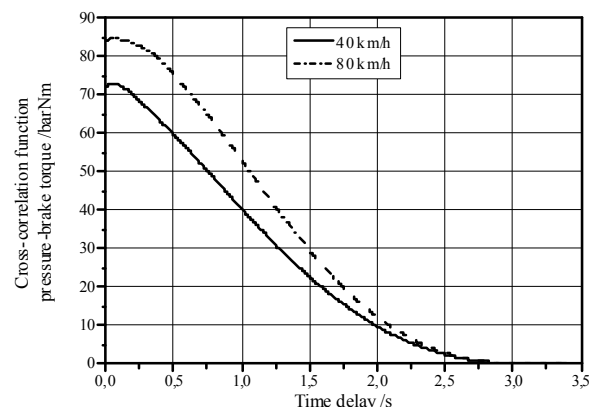


Figure 19 Influence of the initial speed on cross-correlation function between pressure and brake torque (ready-to-drive vehicle)

### 3.4 Cross-spectral density functions

Illustrative examples of magnitudes and phases of the cross-spectral density function between pressure and brake torque are presented in Figs. 20 and 21. It is obvious that the value of the cross-spectral density function magnitude is the largest at low frequency ranges and that it is in the range from 0,12 bar·N·m·Hz ( $f = 3,96$  Hz) to 2994,66 bar·N·m·Hz ( $f = 0,15$  Hz). Values of phase are within the range  $-2,38$  rad ( $f = 3,96$  Hz) to  $3,07$  rad ( $f = 7,62$  Hz).

The analysis of all data obtained during processing shows that the maximum values of cross-spectral density function magnitudes are in the range from 1498,70 bar·N·m·Hz ( $f = 0,15$  Hz,  $v_0 = 60$  km/h, ready-to-drive vehicle) to 5022,17 bar·N·m·Hz ( $f = 0,15$  Hz,  $v_0 = 60$  km/h, fully loaded vehicle). The maximum values of phase are in the range from 2,83 rad ( $f = 6,31$  Hz,  $v_0 = 40$

km/h, fully loaded vehicle) to 3,10 rad ( $f = 5,57$  Hz,  $v_0 = 80$  km/h, ready-to-drive vehicle).

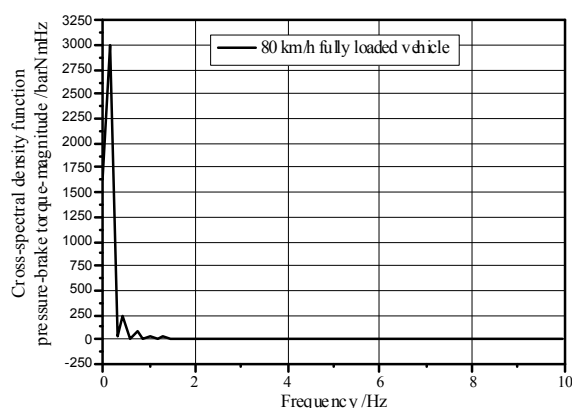


**Figure 20** Magnitude of the cross-spectral density functions between pressure and brake torque

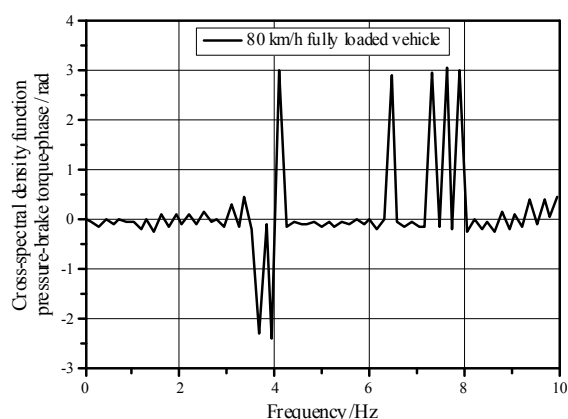


**Figure 21** Phase of the cross-spectral density function between pressure and brake torque

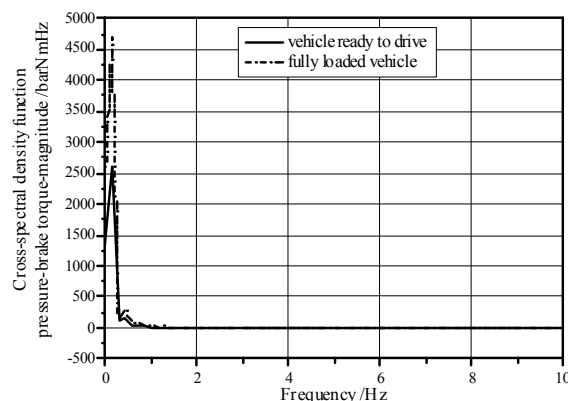


**Figure 22** Influence of the vehicle's weight on the magnitude of cross-spectral density function between pressure and brake torque

The results of analysis of the influence of the vehicle's weight on the magnitude and phase of cross-spectral density function between pressure and brake torque for initial speed of 80 km/h are shown in Figs. 22 and 23. It can be noticed that the increase in vehicle weight affects the increase in maximum value of the magnitude (from 2621,9 bar·N·m·Hz,  $f = 0,15$  to 4685,46 bar·N·m·Hz,  $f = 0,15$  Hz), and that it has small influence on maximum value of cross-spectral density phase between pressure and brake torque (from 2,99 rad,  $f = 3,52$  Hz, ready-to-drive vehicle, up to 3,02 rad,  $f = 2,49$  Hz, for fully loaded vehicle).

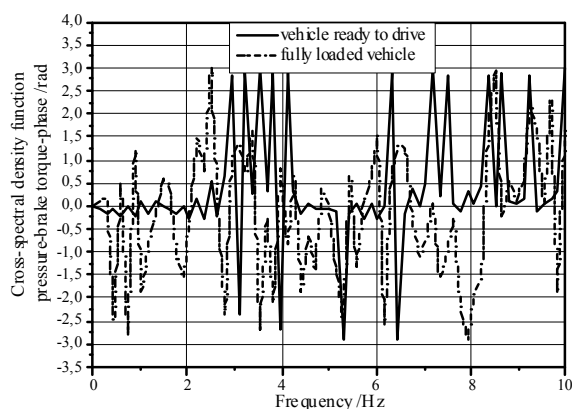


**Figure 23** Influence of the vehicle's weight on the phase of cross-spectral density function between pressure and brake torque

The influence of the initial vehicle speed on magnitude and phase of cross-spectral density function between pressure and brake torque is presented in Figs. 24 and 25. It can be seen that the increase of initial speed of the vehicle affects the increase of maximum value of the magnitude (from 3981,47 bar·N·m·Hz,  $v_0 = 40$  km/h to 4685,46 bar·N·m·Hz,  $v_0 = 80$  km/h at  $f = 0,15$  Hz) and that it has small influence on maximum value of cross-spectral density phase between pressure and brake torque (from 2,98 rad,  $f = 8,21$  Hz, 40 km/h, over 3,02 rad,  $f = 2,49$  Hz, 60 km/h to 3,07 rad,  $f = 7,62$  Hz, 80 km/h).

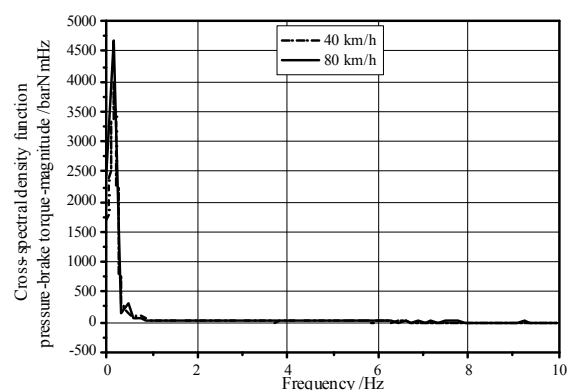


**Figure 24** Influence of the initial speed on the magnitude of cross-spectral density function between pressure and brake torque

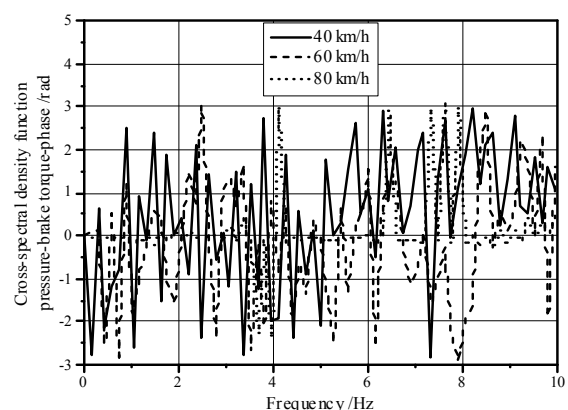


**Figure 25** Influence of the initial speed on the phase of cross-spectral density function between pressure and brake torque

### 3.5 Coherence functions

Analysis of data in Fig. 26 shows that the values of coherence function are in the range from 0,435 to 0,590.

The influence of vehicle's weight in the process of braking until stopping the vehicle is displayed in Fig. 27 for initial speed of  $v_0 = 40$  km/h. Coherence function values are in the range from 0,44 to 0,62 for ready-to-drive vehicle and from 0,455 to 0,75 for fully loaded vehicle.

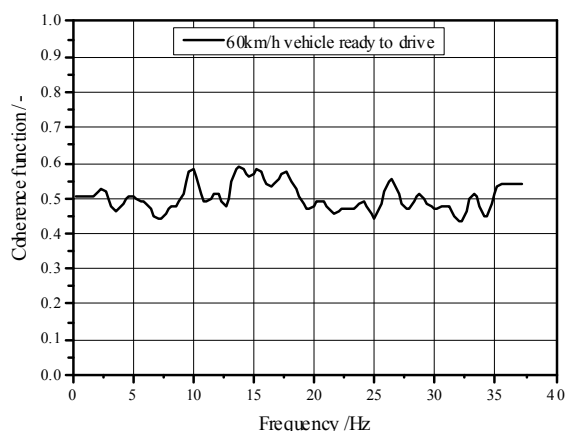


Figure 26 Coherence function between pressure and brake torque

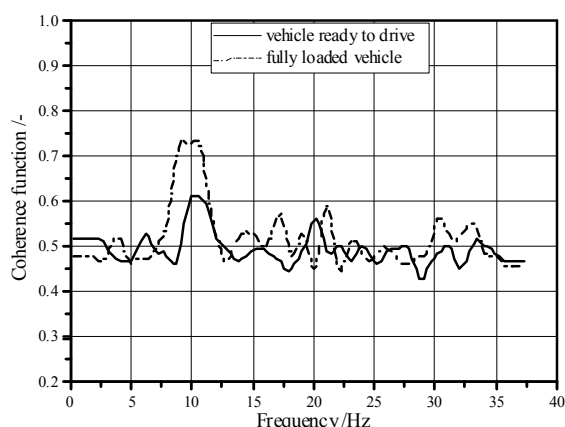


Figure 27 Influence of vehicle's weight on the coherence function between pressure and brake torque

The influence of the initial speed of the vehicle during braking until stopping the vehicle can be seen in Fig. 28. Coherence values are in the ranges from 0,455 to 0,741 ( $v_0 = 40$  km/h), from 0,44 to 0,61 ( $v_0 = 60$  km/h) and from 0,46 to 0,765 ( $v_0 = 80$  km/h).

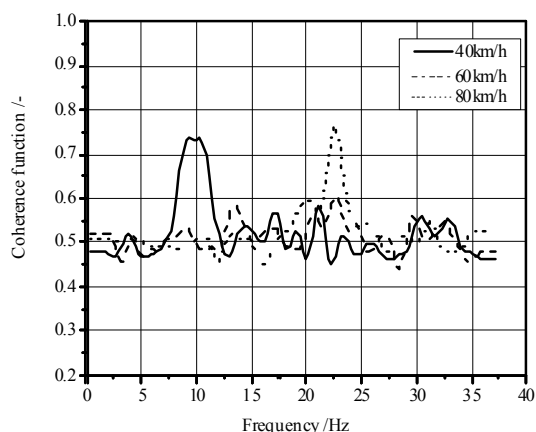


Figure 28 Influence of the initial speed on the coherence function between pressure and brake torque

The obtained data shows that the values of coherence function are in the range from 0,225 ( $f = 31,38$  Hz,  $v_0 = 80$  km/h, ready-to-drive vehicle) to 0,834 ( $f = 22,58$  Hz,  $v_0 = 80$  km/h, fully loaded vehicle). Based on the analysis of all coherence function data, it can be stated that there is a correlation between the brake fluid pressure in the system and the brake torque. This coupling is larger at higher frequencies. Values lower than 1 can be explained by existence of nonlinearities, clearances, noise, etc.

### 3.6 Probability density functions

Fig. 29 illustrates one of the calculated probability density functions for the brake torque as the function of the amplitude for the initial speed of 60 km/h in the case of ready-to-drive vehicle. The maximum value of probability density is 50,98 % and it corresponds to the amplitude of  $-3,0$  N·m and the second peak is at the amplitude 147,0 N·m and value of probability density is 24,12 %.

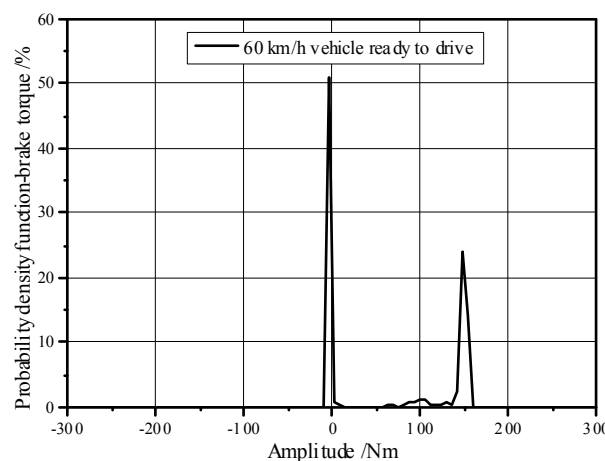


Figure 29 Probability density function of the brake torque as a function of the amplitude

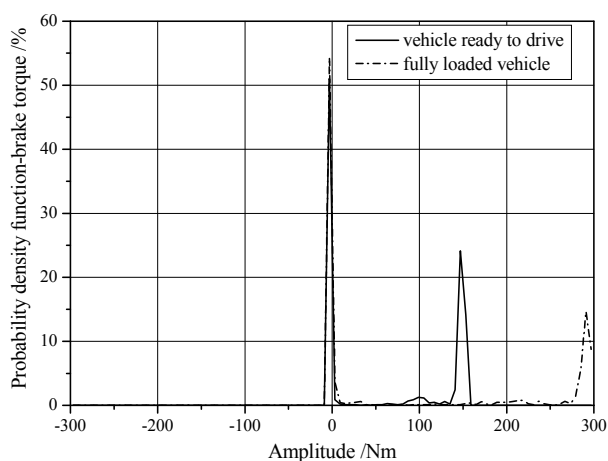
The analysis of obtained data shows that maximum values of probability density function of brake torque are in the range from 50,2 to 58,5 % (amplitude  $-1,0$  N·m,  $v_0 = 40$  km/h, fully loaded vehicle). The analysis of obtained data shows that maximum values of probability density function-pressure are in the range from 50,0 % (amplitude  $-3,0$  bar,  $v_0 = 80$  km/h, fully loaded vehicle) to 65,23 % (amplitude  $-3,0$  bar,  $v_0 = 40$  km/h, fully loaded vehicle).

Influence of changes of the vehicle's weight on probability density of brake torque for the initial speed of 60 km/h is shown in Fig. 30. The maximum value of the probability density varies within the limits of 50,98 % for the amplitude of  $-3,0$  N·m for ready-to-drive vehicle, up to 54,30 % for fully loaded vehicle, which corresponds to the same amplitude of the  $-3,0$  N·m.

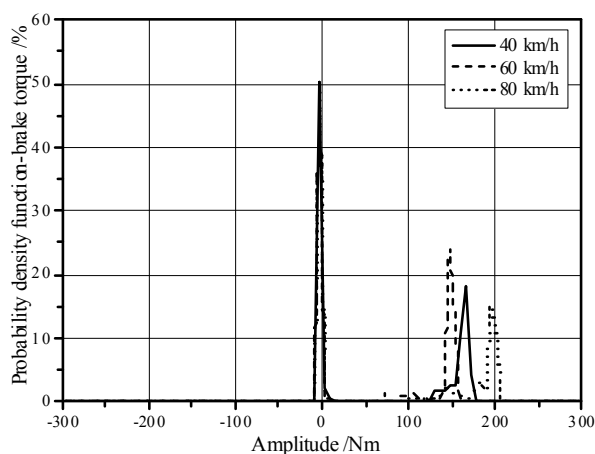
The influence of initial velocity in the braking process on probability density of brake torque is shown in Fig. 31. Maximum values are practically identical and they are within the limits of 50,39 % for amplitude  $-3,0$  N·m and initial speed 40 km/h, over 50,98 % in amplitude  $-3,0$  N·m and initial speed 60 km/h, back to 50,39 % for amplitude  $-3,0$  N·m and initial speed 80 km/h. The second peaks change from 18,16 % ( $v_0 = 40$  km/h, amplitude 165,0 N·m), over 24,12 % ( $v_0 = 60$  km/h,



amplitude 147,0 N·m) to 15,92 % ( $v_0 = 80$  km/h, amplitude 195,0 N·m).

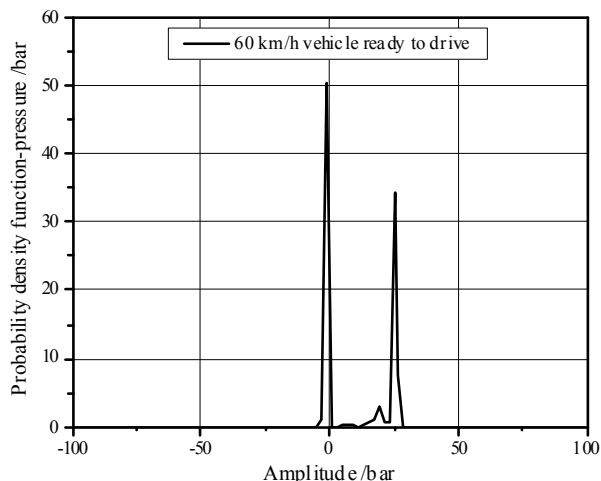


**Figure 30** Influence of vehicle's weight on the probability density of the brake torque



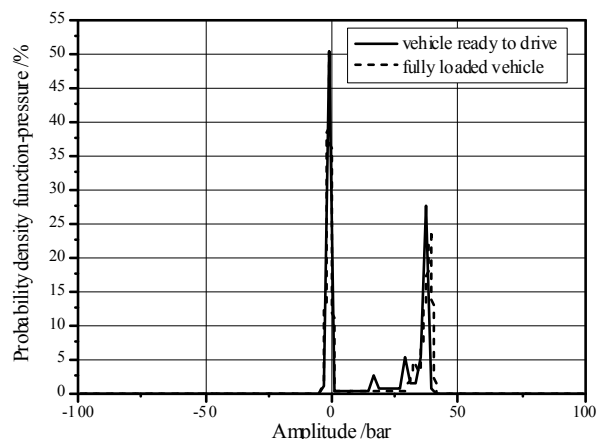
**Figure 31** Influence of initial speed on the probability density of the brake torque

Fig. 32 illustrates one of the calculated probability density functions of pressure as the function of the amplitude for initial speed of 60 km/h, in the case of ready-to-drive vehicle. The maximum value of the probability density is 50,29 % and it corresponds to the amplitude of -1,0 bar.



**Figure 32** Probability density function of the pressure as a function of the amplitude

The influence of vehicle's weight on the value of the probability density of pressure for the initial speed of 40 km/h is shown in Fig. 33. The maximum values of the probability density are identical for ready-to-drive vehicle and for fully loaded vehicle (50,2 %, which corresponds to the amplitude of the -1,0 bar).



**Figure 33** Influence of vehicle's weight on the probability density of the pressure

Analysis of the effects of initial velocity in the braking process on probability density of pressure (Fig. 34) shows that the maximum values are identical for all initial speeds (50,2 %, which correspond to the amplitude of the -1,0 bar). The second peaks change from 17,48 % ( $v_0 = 40$  km/h, amplitude 47,0 bar), over 26,76 % ( $v_0 = 60$  km/h, amplitude 49,0 bar) to 23,24 % ( $v_0 = 80$  km/h, amplitude 39,0 bar).

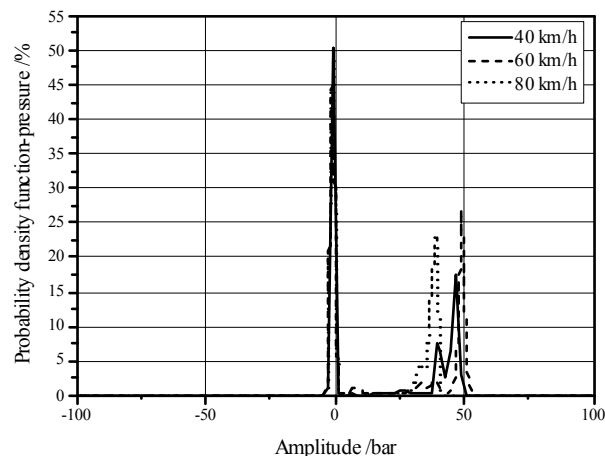


**Figure 34** Influence of initial speed on the probability density of the pressure

### 3.7 The transfer functions

Illustrative diagram of the transfer function of the pressure-brake torque in the frequency domain for the initial speed of 80 km/h and ready-to-drive vehicle is shown in Fig. 35. Transfer function values are in the range from 0,632 N·m/bar ( $f = 32,26$  Hz) to 56,02 N·m/bar ( $f = 25,22$  Hz).

The obtained data show that the values of transfer function are in the range from 0,273 N·m/bar ( $f = 32,845$  Hz,  $v_0 = 40$  km/h, ready-to-drive vehicle) to 83,48 Nm/bar ( $f = 8,5$  Hz,  $v_0 = 60$  km/h, ready-to-drive vehicle).

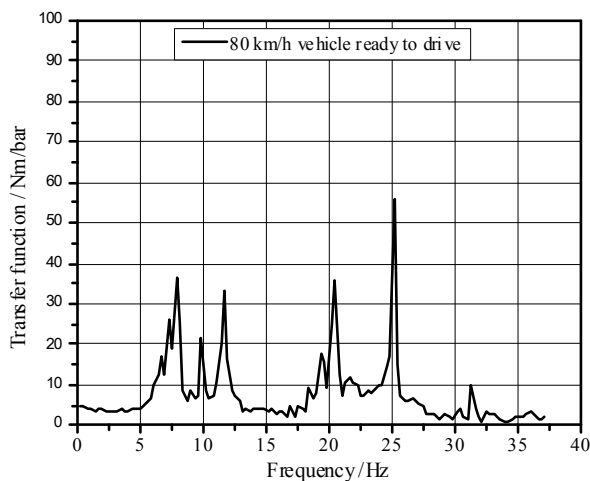


Figure 35 Transfer function between pressure and brake torque

By considering the influence of the vehicle's weight on transfer functions for the initial speed of braking of 80 km/h (Fig. 36), it is apparent that there is a slight decrease of the maximum value of transfer function, which is in the range from 0,441 N·m/bar ( $f = 32,26$  Hz) to 83,48 N·m/bar ( $f = 8,504$  Hz) for ready-to-drive vehicle and is in the range from 0,643 N·m/bar ( $f = 34,605$  Hz) to 78,776 N·m/bar ( $f = 7,918$  Hz) for the fully loaded vehicle.

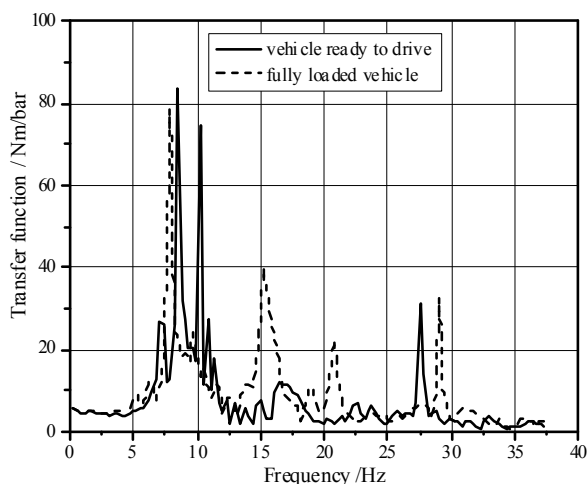


Figure 36 Influence of vehicle's weight on the transfer function between the pressure and brake torque

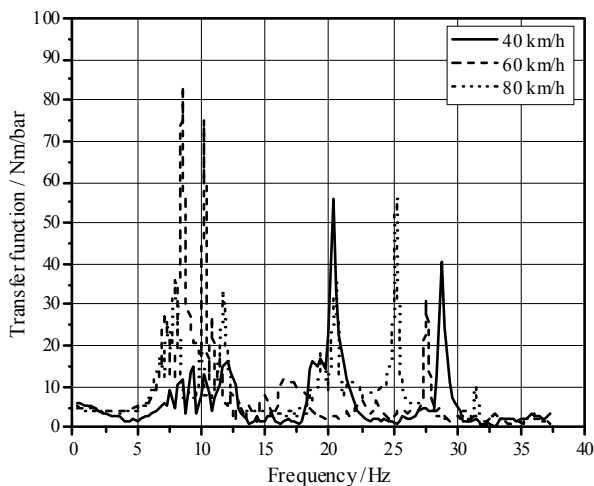


Figure 37 Influence of initial speed on the transfer function between the pressure and brake torque

Effects of initial velocity of the braking process on the transfer function pressure-brake torque (Fig. 37) lead to changes in value which varies within the range of 1,692 N·m/bar ( $f = 4,399$  Hz) to 55,926 N·m/bar ( $f = 20,235$  Hz) for the initial speed of 40 km/h, from 0,441 N·m/bar ( $f = 32,259$  Hz) to 83,48 N·m/bar ( $f = 8,504$  Hz) for the speed of 60 km/h, 0,632 N·m/bar ( $f = 32,259$  Hz) to 56,021 N·m/bar ( $f = 25,22$  Hz) for the initial speed of 80 km/h, all this in case of fully loaded vehicle.

### 3.8 Probability functions

Illustrative examples of probability functions of torque and pressure in the function of amplitude at an initial speed of 40 km/h and for ready-to-drive vehicle are given in Figs. 38 and 39. The maximum value of 1,0 of the probability function of pressure is achieved at the amplitude of 25,0 bar and probability function of torque is achieved at amplitude of 171,0 N·m.

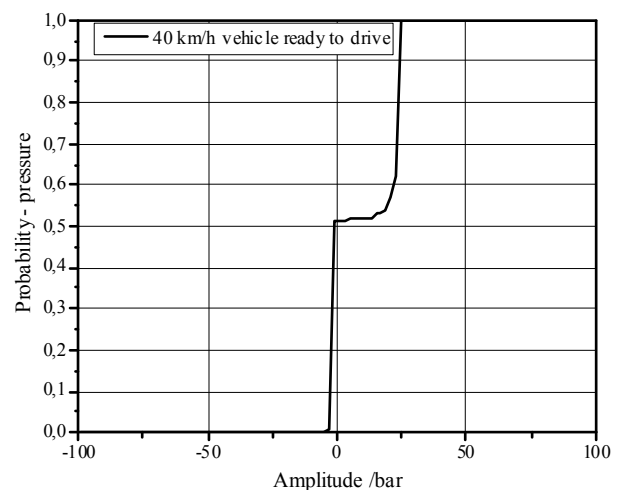


Figure 38 The probability-pressure as function of amplitude

By analysis of the influence of vehicle's weight on the probability function of brake torque (Fig. 40) for the initial vehicle speed of 60 km/h, it can be concluded that the probability function reaches value 1,0 for the value of the amplitude of torque of 153,0 N·m, for ready-to-drive vehicle, and of 297,0 N·m for the fully loaded vehicle.

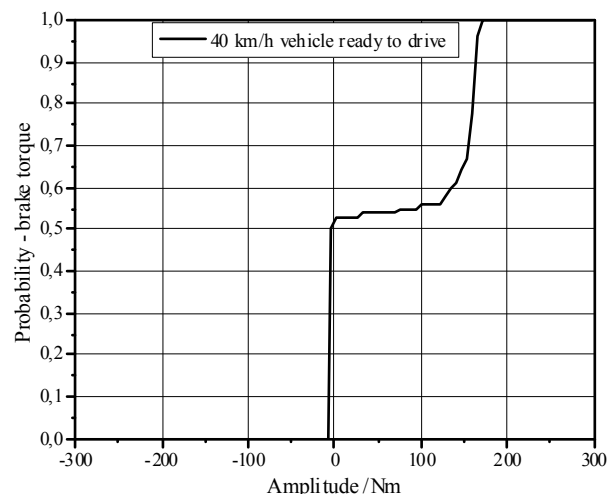
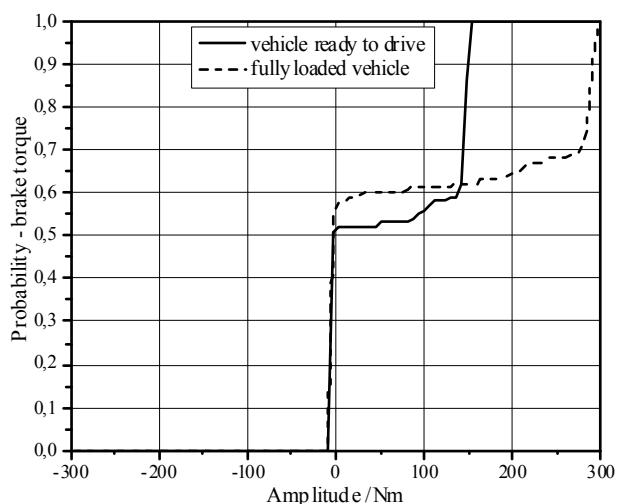
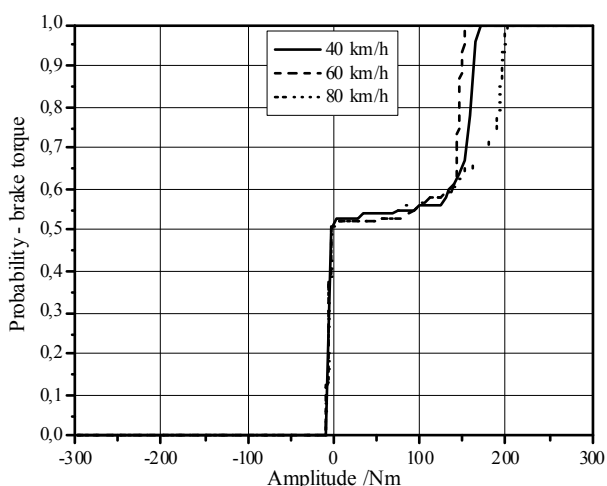


Figure 39 Probability-torque as function of the amplitude



**Figure 40** The influence of the vehicle's weight on the probability function-torque

Based on diagram in Fig. 41, it can be concluded that the probability function reaches value 1,0 for the value of the amplitude of torque of 171,0 N·m, for initial speed  $v_0 = 40$  km/h, of 153,0 N·m for initial speed  $v_0 = 60$  km/h, of 201,0 N·m for initial speed  $v_0 = 80$  km/h. A ready-to-drive vehicle was considered.



**Figure 41** Influence of initial speed on the probability function-torque

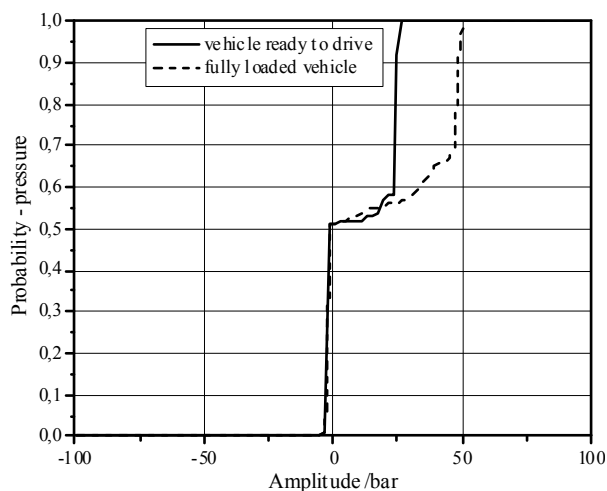


**Figure 42** The influence of the vehicle's weight on the probability function-pressure

From the analysis of the influence of vehicle's weight on the probability function-pressure (Fig. 42), for the initial vehicle speed 60 km/h, it can be concluded that probability-pressure function reaches 1,0 at the amplitude of 27 bar, for ready-to-drive vehicle and at the amplitude 51 bar, for fully loaded vehicle.

By analysing the diagram in Fig. 43, it can be concluded that probability function-pressure reaches the value of 1,0 at the amplitude of pressure of 49,0 bar, for initial speed of 40 km/h, and for amplitude of 51,0 bar and for speeds 60 km/h and for amplitude of 39,0 bar and for speeds 80 km/h. A fully loaded vehicle is considered here.

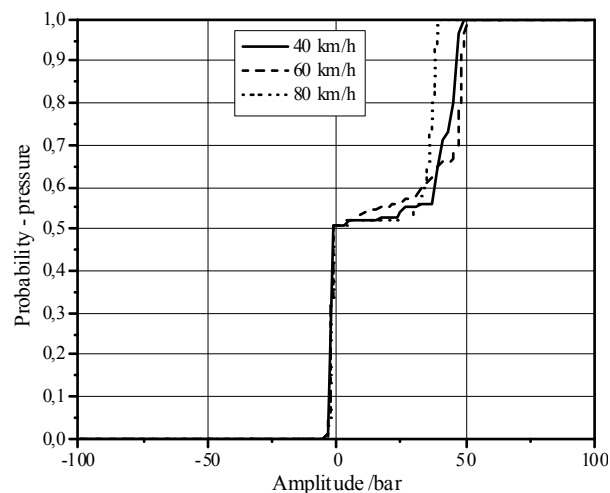


**Figure 43** Influence of initial speed on the probability function-pressure

### 3.9 Density of mutual probability

The density of mutual probability as a function of pressure and brake torque for initial speed of 80 km/h and for ready-to-drive vehicle is shown in Fig. 44. The maximum value is 0,732 %. Density of mutual probability varies within the limits from 0,146 ( $v_0 = 40$  km/h, fully loaded vehicle) to 0,977 ( $v_0 = 80$  km/h, fully loaded vehicle).

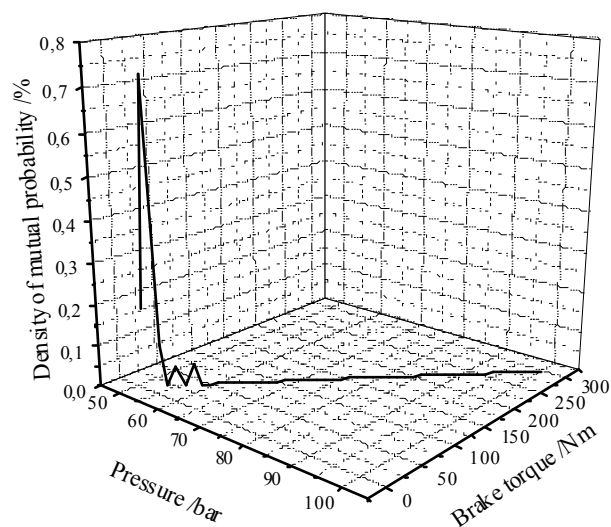


**Figure 44** Density of mutual probability for an initial speed of 80 km/h and the vehicle that is ready-to-drive

## 4 Conclusion

Based on the conducted research, the following can be concluded:

- 1) The developed methodology of experimental research of mechanical properties of drum brakes can be applied with sufficient reliability in practice.
- 2) Data processing methods used in this paper allow the analysis of actual mechanical characteristics of drum brakes during operation.
- 3) The obtained results indicate a nonlinear transformation of the brake fluid pressure into the brake torque and a significant influence of the parameters of the vehicle's weight and initial speed of the vehicle observed at the beginning of the transient process. Based on the analysis of all data on coherence function, it can be stated that, in the presented system, there is a correlation between the brake fluid pressure in the brake system and the brake torque. This coupling is larger at higher frequencies. Values lower than 1,0 are explained by existence of nonlinearities, clearances, noise, etc. By considering the influence of the vehicle's weight on the transfer functions, it may be concluded that apparently there is a slight decrease of the value of transfer function. Changing the initial velocity of the braking process has influence on the transfer function pressure-brake torque, where the maximum values correspond to initial velocity of 60 km/h.

## Acknowledgment

This paper is part of the research included in the project: "The research of vehicle's safety as part of the cybernetic system: the driver-vehicle-environment", supported by the Ministry of Education, Science and Technological Development of the Republic of Serbia. The authors would like to thank the Ministry for the financing of this project.

## 5 References

- [1] Todorovic, J. Braking of motor vehicles, Institute for textbooks and scientific resources, Belgrade, Serbia, 1988. (in Serbian)
- [2] Demeć, M.; Lukic, J. Motor vehicles theory of movement, monograph, Faculty of Mechanical Engineering, Kragujevac, Serbia, 2011 (in Serbian)
- [3] Newcomb, T. P.; Spurr, R. T. Braking of road vehicles, Chapman and Hall, London, 1967.
- [4] Day, A. J. Drum Brake Interface Pressure Distributions. // Proceedings of the Institution of Mechanical Engineers, Part D: Journal of Automobile Engineering, April 1991 205: pp. 127-136.
- [5] Ioannidis, P.; Brooks, P. C.; Barton, D. C. Drum Brake Contact Analysis and Its Influence on Squeal Noise Prediction, SAE Paper 2003-01-3348, 2003.
- [6] Day, A. J.; Harding, P. R.; Newcomb, T. P. Combined thermal and mechanical analysis of drum brakes. // Proc. IMechE, 198, 4(1984), pp. 287-294.
- [7] Newcomb, T. P.; Day, A. J. Finite element analysis of drum brake performance, Int. Seminar Autom. Brake Components, IMechE, Birmingham, 1985.
- [8] Drum Brake and Actuation Systems-Unbeatable Safety, Retrieved September 19, 2012, from

<http://www.trwaftermarket.com/en/Products/Drum-Brake-and-Actuation-Systems/>

- [9] Glisovic, J.; Radonjic, R. Evaluation of drum brake's characteristics for motor vehicles. // Proceedings of IRMES, Jahorina, Bosnia and Herzegovina, 2002, pp. 769-774. (in Serbian)
- [10] Glisovic, J. Identification of transfer characteristics of drum brakes, M.Sc. Dissertation, Faculty of Mechanical Engineering, Kragujevac, Serbia, 2001. (in Serbian)
- [11] Demeć, M.; Miric, N. Contribution to the definition of the vehicle's dynamic model to analyze the braking process. // Zastava, 30, (1991). (in Serbian)
- [12] Bendat, J.S.; Piersol, A.G. Engineering Applications of Correlation and Spectral Analysis, John Wiley and Sons, London, 1980.
- [13] Bendat, J. S. Nonlinear Systems-Techniques and Applications, John Wiley and Sons, London, 1998.
- [14] Bendat, J. S.; Piersol, A. G. Random Data Analysis and Measurement Procedures, John Wiley and Sons, London, 2000.
- [15] Demeć, M. ANALSIGDEM – Software for signal analysis, [www.ptt.yu/korisnici/i/m/imizm034/](http://www.ptt.yu/korisnici/i/m/imizm034/) (2003).
- [16] Demeć, M. DEMPARCHO – Software for partial coherence function calculation, [www.ptt.yu/korisnici/i/m/imizm034/](http://www.ptt.yu/korisnici/i/m/imizm034/) (2003).
- [17] Demeć, M. Contribution to determining the reliability of new method for identification of motor vehicles' oscillatory parameters. // Vojnotehnički glasnik, 2, (1997), pp. 135-146. (in Serbian)
- [18] Demeć, M. Cybernetic system: man-vehicle-environment, Center for Scientific Research of SANU and University of Kragujevac, monograph, 2008. (in Serbian)

## Authors' addresses

### **Demeć Miroslav, PhD., Full Professor**

University of Kragujevac  
Faculty of Engineering  
Sestre Janjic 6  
34000 Kragujevac, Serbia  
Contact Tel. ++38134330487 / Fax. ++38134333192,  
E-mail: [demic@kg.ac.rs](mailto:demic@kg.ac.rs)

### **Glisović Jasna, PhD., Assistant Professor**

University of Kragujevac  
Faculty of Engineering  
Sestre Janjic 6  
34000 Kragujevac, Serbia  
Contact Tel. ++38134335990 ext. 707 / Fax. ++38134333192,  
E-mail: [jaca@kg.ac.rs](mailto:jaca@kg.ac.rs)

### **Miloradović Danijela, PhD., Assistant Professor**

University of Kragujevac  
Faculty of Engineering  
Sestre Janjic 6  
34000 Kragujevac, Serbia  
Contact Tel. ++38134335990 ext. 687 / Fax. ++38134333192,  
E-mail: [neja@kg.ac.rs](mailto:neja@kg.ac.rs)

### **Lukić Jovanka, PhD., Full Professor**

University of Kragujevac  
Faculty of Engineering  
Sestre Janjic 6  
34000 Kragujevac, Serbia  
Contact Tel. ++38134335990 ext. 701 / Fax. 38134333192,  
E-mail: [lukicj@kg.ac.rs](mailto:lukicj@kg.ac.rs)